Efficient Raman laser based on a CaF_2 resonator

Ivan S. Grudinin[1,*] and Lute Maleki[1,2]

[1]*Jet Propulsion Laboratory, California Institute of Technology, 4800 Oak Grove Drive, Pasadena, California 91109, USA*
[2]*OEwaves, 1010 East Union Street, Pasadena, California 91106, USA*
[*]*Corresponding author: grudinin@caltech.edu*

Received December 7, 2007; accepted January 9, 2008;
posted February 14, 2008 (Doc. ID 90479); published March 27, 2008

We report on an ultralow-threshold Raman laser based on a CaF_2 whispering-gallery-mode resonator. The laser is demonstrated to have a conversion efficiency above 60%. The observed low lasing threshold is made possible by the ultrahigh optical quality factor of the cavity, which is on the order of $Q=10^{10}$. The laser is fiber-compatible and is fabricated with a very simple technique. We also demonstrate a single-mode operation of the laser in a multimode cavity as well as a multimode operation of the laser in a single-mode cavity. © 2008 Optical Society of America

OCIS codes: 140.3550, 160.4330, 190.5650, 230.5750.

The Raman scattering effect was experimentally discovered by Raman and Krishnan [1] in liquids and independently by Landsberg and Mandelshtam in crystals [2]. Lasers based on the stimulated Raman scattering (SRS) effect have found numerous applications in material science, molecular spectroscopy, and in many biological studies. SRS can be used to convert one optical frequency into another, making it possible to access virtually any wavelength within the Raman-active material's transparency window. Whispering-gallery-mode resonators (WGMRs) are ideally suited for Raman laser applications as they are compact and fiber-compatible. Their high optical Q factors make it possible to easily achieve high intracavity power to enhance nonlinear effects [3–7].

Fused-silica microsphere and microtoroid as well as crystalline WGMR Raman lasers have been previously demonstrated [8,9]. In this paper we show that by using a very simple fabrication technique, it is possible to obtain a very high Q-factor crystalline fluorite resonator as a Raman laser. This laser operates as a fiber-compatible device with a bidirectional conversion efficiency exceeding 60%. We also demonstrate the single-mode operation of a laser based on a multimode cavity and multimode operation of a laser based on a single-mode cavity.

Fluorite cavities have certain advantages over their fused-silica counterparts. The lower loss of the crystalline material allows for higher Q factors and the associated intracavity optical power buildup, which along with a higher Raman gain of the fluorite [10] lead to lower thresholds of Raman lasing. This material may easily be superpolished to subnanometer surface roughness as previously demonstrated [11], and the resulting surface is immune to water vapor absorption in contrast to the fused-silica's surface. The refractive index of fluorite is smaller than that of fused-silica, making it possible to use common optical fibers to couple light in and out of the cavity. Using an optical fiber, a coupling efficiency exceeding 80% is routinely achieved in our laboratory. Finally, it is possible to use diamond machining techniques to produce fluorite cavities with a predesigned spectral response and single-mode cavities [12].

We have used a very simple polishing technique to fabricate a WGMR out of a CaF_2 crystal. A small cylinder was initially cut from a UV-grade CaF_2 blank obtained from Edmund Industrial Optics. The cylinder was glued onto a cap that was then installed onto a high-speed motor and a thin thread with a diamond abrasive was used to create a region that supports the whispering-gallery modes (WGMs). It is worth noting that such a technique can be automated, and disks with a curvature radius down to 10 μm and below may be produced using this technique.

Angle-polished fiber couplers were used to pump the laser and monitor its output. The couplers were similar to those presented in [13] and were made by cleaving the fiber at a right angle followed by angle-polishing. Such a coupler has a phase-matching evanescent field region to couple light to the WGMs of the resonator. In our case the fluorite resonator was 5 mm in diameter and the angle of the coupler was ~10°. We have used a single-mode fiber P3-980A-FC-5 from Thorlabs to fabricate couplers. An example of the coupler and the resonator profile are shown in Fig. 1. A narrow linewidth Nd:YAG laser manufactured by Lightwave Electronics (now JDSU) emitting light at 1064 nm was used to excite the WGMs in the cavity. A simplified Pound–Drever–Hall (PDH) [14] locking technique allowed us to continuously pump the WGM of the cavity, and the resulting Raman emission was monitored in a cw mode. Simplified schematics of the setup are shown in Fig. 2. To implement a PDH frequency lock, the pump beam was phase-modulated at 0.6 MHz with a resonant electro-optical modulator (EOM) and the WGM cavity acted as a frequency discriminator. The amplitude of the reflected portion of the pump beam, produced at the

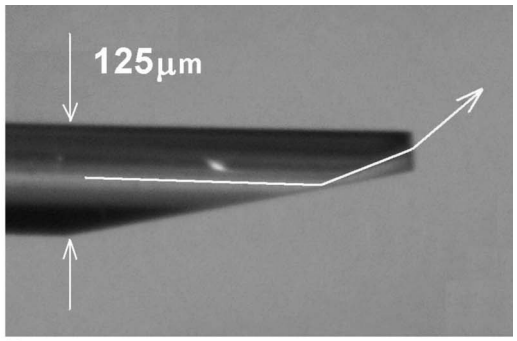

(a)

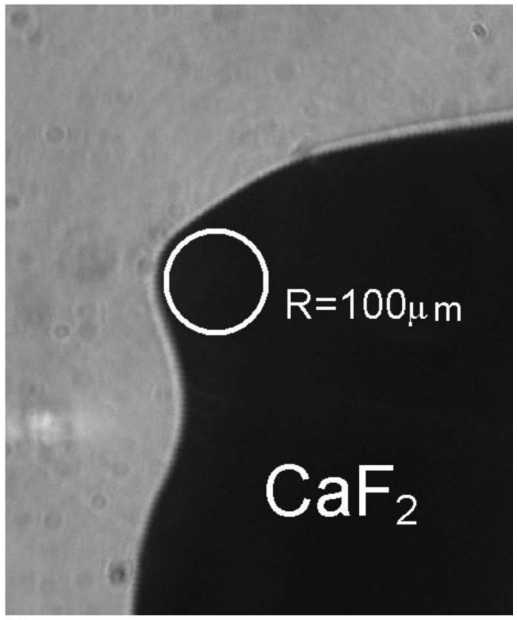

(b)

Fig. 1. (a) Angle-polished fiber coupler. Single-mode fiber is polished at an angle, which was computed to optimize coupling to a 5 mm CaF_2 disk. An approximate ray path is shown with a white arrow. (b) Shadow photograph of a CaF_2 resonator. The white circle shows that the radius of curvature of the disk in the WGM localization area is ~100 μm.

output of the coupler A, contains a component at the modulation frequency. This component was recorded by a Thorlabs photodetector DET10C and multiplied by a phase-shifted modulation signal with the help of a mixer to obtain the PDH error signal. Phase-shifting, used to optimize the error signal, was achieved by varying the frequency of excitation of the resonance transformer in the phase modulator. The error signal was amplified and filtered with a low-noise voltage amplifier SR560 and fed back to the laser piezo. Typical error, transmission, and reflection signals for the cases of linear modes are shown in Fig. 3. The pumping of the Raman laser was performed by the same mode that is used for frequency-locking. It should be noted that the observed WGMs were non-Lorentzian, as thermal and Kerr nonlinearities were present at the level of power that was used. Nevertheless, the error signal still had the linear region that allowed us to successfully lock the laser. When the laser was frequency locked to a cavity, the amplitude noise of the reflected signal was ~20%, which may be significantly reduced by upgrading the servo.

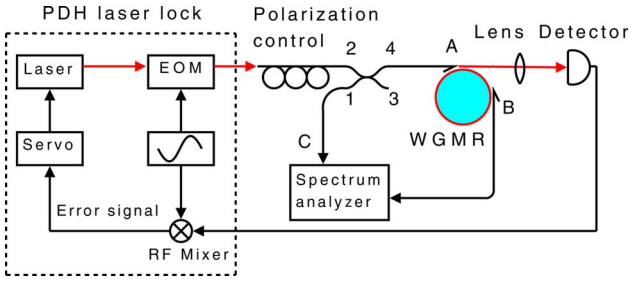

Fig. 2. (Color online) Setup diagram. A PDH locking technique is used to stabilize the power in a cavity; A and B denote input and output angle-polished fiber couplers.

When a resonator is pumped, the Raman gain is created symmetrically for the counterpropagating sets of WGMs. It may be argued that the coupling losses seen by each of the modes in the pair of counterpropagating modes might be different due to the asymmetry of the refractive index inside the angle-polished fiber coupler. However, coupling losses are defined by the overlap integral between the cavity mode and the field configuration in the fiber and do not depend on the sign of the wave vector, as the WGMR is linear and symmetrical [15,16]. We assume that the power in each of the Raman lasing modes of a pair is equal. The lasing linewidth, or coherence of the pair of lasers, could in principle be measured by recording a beat note of the pair of modes on the photodetector.

The two fiber couplers and the reflection port (90/10 coupler) were used to monitor these two laser outputs simultaneously. The free beam formed by the coupler A suffered attenuation from reflection loss at the cleaved fiber, lens, and detector surfaces. If we assume these losses to be 4% each, which corresponds to a reflection coefficient at a glass surface, then the power inside the fiber is higher than that observed at the detector by a factor of $\simeq(0.96)^{-4}=1.18$. This correction is taken into account in the following estimates.

The maximum measured coupling efficiency was above 70% for the input A and above 80% for the output B coupler. It is worth noting that critical coupling approaching

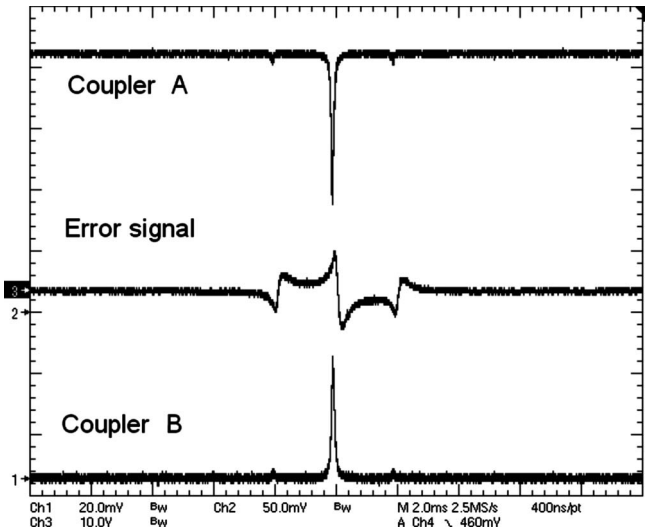

Fig. 3. Optical power from coupler A (channel 2), B (channel 1) recorded with the photodetectors and the error signal.

100% may be achieved for the WGMRs. The intrinsic optical Q factor of the WGM, measured at a pump wavelength of 1064 nm, is found to be $(6.9\pm0.7)\times10^9$. This value was derived from the linewidth ($\simeq$40.5 kHz) of the mode resonances in the undercoupled regime when no Raman lasing was present. A splitting of ~135 kHz caused by the Rayleigh scattering-induced coupling between the counterpropagating modes was also observed. In a particular measurement, the mode was pumped so that the input coupler transmission loss was ~244 μW. This does not include the forward Stokes power that was emitted at a different angle and missed the detector. The maximum achievable coupling for the WGM corresponded to a 277 μW transmission loss or ~50% of the coupler transmission. Figure 4 shows power spectra of the transmitted and reflected optical signals as seen on the spectrum analyzer Yokogawa AQ6319. A transmission ratio of 4 to 1 direction of the reflection port was measured to be 0.0145 at the pump wavelength, so the reflected power measured with a spectrum analyzer was adjusted accordingly to give the optical power values in the fiber. The 90/10 coupler was designed for 1550 nm, so the actual transmission ratios at the wavelength of 1064 nm were different from 90% and 10%. From Fig. 4 it can be seen that there is 14 μW of reflected pump laser radiation and 80 μW of backward Stokes radiation shifted by 9.72 THz (38 nm) from the pump laser frequency. From the forward coupler we see that the power of the pump laser and the Stokes component are equal, and since Raman lasing is symmetrical for counterpropagating modes, we derive the forward lasing Stokes and pump laser power of 80 μW. This adds up to 254 μW, which is the total power loss in the cavity within the experimental uncertainty. Thus the bidirectional Raman conversion efficiency for this particular mode is $100\%\times160/244=65\%$. As compared to the 24% unidirectional efficiency in [9] observed when eight cascaded lasing multimode Stokes components were present, the 32% unidirectional efficiency in this paper is observed for the single-lasing Stokes component and near-single-mode operation.

The threshold of Raman lasing in a WGM cavity is given by the following equation [17]:

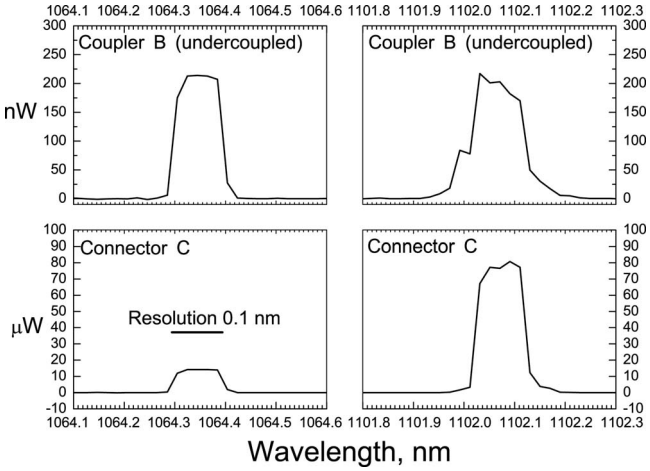

Fig. 4. Spectra of input and output power as recorded by the coupler B and the fiber connected to output 4 of the port. See Fig. 2 for details.

$$P_{th}=\frac{\pi^2n^2}{\xi g_c Q_S Q_P}\frac{V_m}{\lambda_P\lambda_S}. \quad (1)$$

Here n is the refractive index, and Q_P and Q_S are cavity quality factors for the pump and Stokes wavelengths λ_P and λ_S, respectively. The cavity Raman gain g_c is equal to the bulk Raman gain. V_m is the WGM volume, and ξ accounts for noncritical coupling and an imperfect overlap of the pump and Raman WGMs. The refractive index of fluorite at the pump and Stokes wavelength is 1.43, and the mode TE_{ll1} of a 5 mm cavity has a volume of 2.7×10^{-12} m^3. We assume Q_S and Q_P to be 3.5×10^9 and the Raman gain coefficient to be 2.4×10^{-13} m/W [10]. These values give a Raman threshold of 16 μW for $\xi=1$, comparable to the measured threshold of 78 μW. This discrepancy may be explained if we assume that the excited mode was not a fundamental TE_{ll1} mode but rather a mode with a larger effective volume. The threshold would increase with an increase in volume of the mode. Additionally, the intermodal coupling that is responsible for the counterpropagating mode splitting also leads to the reduction of the intracavity power buildup by a factor of 2 in the case of strong modal coupling [8]. The factor ξ in Eq. (1) is <1, as the coupling and modal overlap are not ideal.

From additional measurements it was found that the spectrum of Fig. 4 typically consists of several lasing Stokes WGMs as presented in Fig. 5(a). The strongest lasing mode exceeds the other modes by at least 15 dB, nearly making it a single-mode lasing spectrum. Figure 5(b) presents a similar measurement on a linear scale. Only forward Stokes emission was recorded, making it impossible to obtain the efficiency. The spectra in Fig. 5 were obtained for different pumping WGMs with an intrinsic Q factor of 7×10^9 for the upper spectrum and 10^{10} for the lower spectrum. It is seen that the lasing modes are separated by the resonator free spectral range (FSR), so that only the modes from a particular family of modal indices lmq, with different l and similar $l-m$, are lasing. The number of lasing modes was experimentally found to depend on loading conditions and the modal Q factor. Increasing the Q factor reduced the number of peaks in the spectrum. Even though the spectrum of our multimode cavity is rich with higher-order azimuthal modes, the combination of a high Q factor and a narrow Raman gain made it possible to observe single-mode lasing. In these measurements the Stokes power was equal to the pump power in the forward direction, as monitored by the output coupler in the undercoupled regime. The spectrometer's resolution in Fig. 5 is 0.012 nm and the cavity's FSR is 0.049 nm.

It was shown in [18] that the millimeter-sized cavity may have its mode frequency relatively stable at the 10^{-12} level in 1 s, which corresponds to 300 Hz if the wavelength is 1 μm. Thus one may expect the Raman laser to be relatively stable and have a narrow linewidth.

We have also observed Stokes lasing modes in a special single-mode cavity. This cavity is a cylinder on which a small 5 μm $\times$ 3 μm waveguide is formed with a diamond turning process. Such a waveguide supports only one WGM per cavity FSR. Although many Stokes modes separated by the cavity's FSR were found to be lasing [Fig.

6(b)] in this resonator at a pump power of 2.4 mW, a true single-mode operation may be achieved if the Q factor is high enough and mode competition for the Raman gain is strong. The multimode lasing in a single-mode cavity may be explained by weak mode competition. The loaded Q factor of $\sim 4\times 10^8$, intrinsic $Q=(7.2\pm 0.1)\times 10^8$, was too low for any specific mode to consume all the available Raman gain. Our diamond turning apparatus was not accurate enough to provide the single-mode cavity with a Q factor higher than 10^9. The application of a more elaborate diamond turning process should enable higher Q factors and thus a true single-mode operation of a Raman laser based on a single-mode fluorite cavity. The sidebands on the pump laser spectra [Fig. 6(a)] were only observed in the forward direction. These weak features might be explained by four-wave mixing between the pump and the Stokes components.

The power that can be obtained from our Raman laser is limited by the Kerr and thermal nonlinearities and cascaded Raman lasing process. Increasing the power in the pump mode leads to cascaded lasing, where higher-order Stokes components appear, which limits the efficiency of a single-mode operation. Nonlinearities also make the shape of the cavity mode significantly different from a Lorentzian, thus the PDH locking technique is no longer reliable. If a higher power is required, a WGM with a larger volume must be selected.

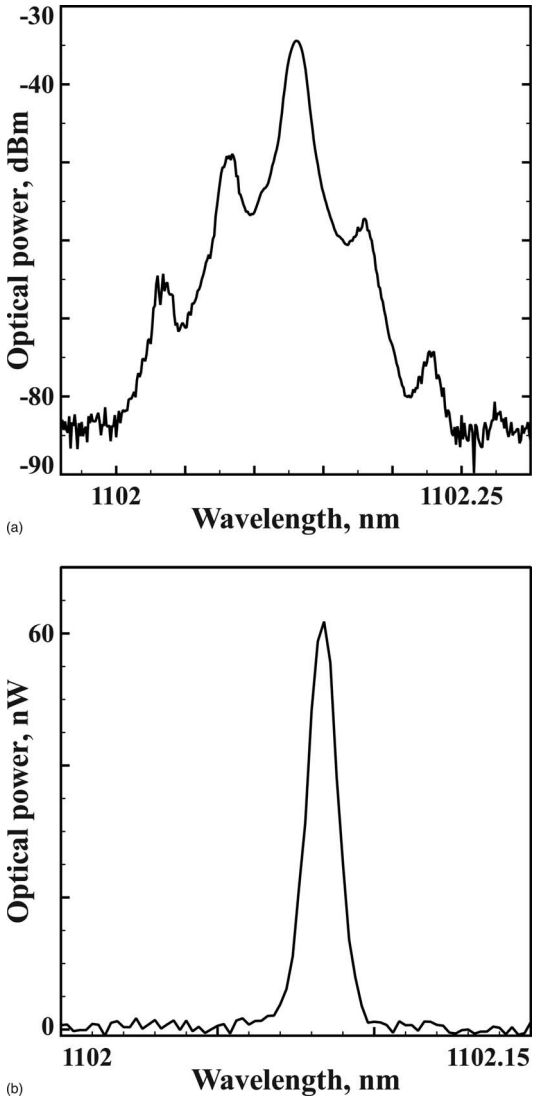

Fig. 5. Optical power spectrum of a lasing Stokes component on (a) log-linear and (b) linear scales. Spectra were recorded for two different pumping WGMs. Optical power is not calibrated.

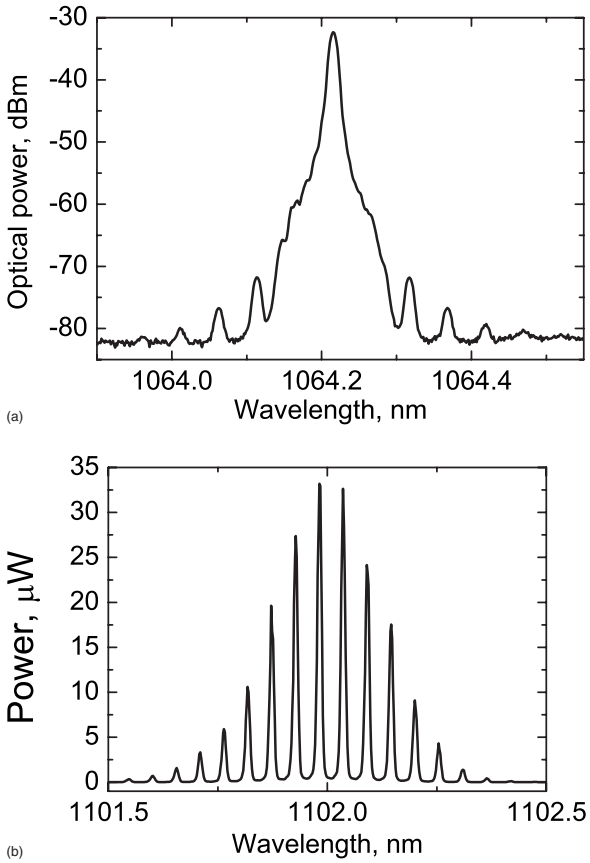

Fig. 6. (a) Pump and (b) Stokes spectra for the single-mode WGMR. Resolution is 0.01 nm; pump power is 2.4 mW. Approximately 40 lasing modes were observed above the noise level.

In conclusion, we have demonstrated a Raman laser based on a fluorite WGM cavity with a threshold at the microwatt level, high efficiency, and single-mode operation. Fiber compatibility of our laser may be utilized in compact and efficient optoelectronic devices. One way to increase the power output of the Raman laser is to use WGMs with a larger volume. A high Q-factor single-mode WGMR may be used to generate a single-mode emission. Alternatively, a smaller cavity with a near-single-mode spectrum and high Q factor may be used. Single-mode Raman emission is useful in many spectroscopic applications. Additionally, the multimode emission could be used to generate relatively stable gigahertz-range beat-note signals.

ACKNOWLEDGMENTS

This research was performed at the Jet Propulsion Laboratory, California Institute of Technology, under a contract with NASA, with support from the Defense Ad-

vanced Research Projects Agency's Analog Optical Signal Processing Program. The authors acknowledge useful discussions with A. B. Matsko.

REFERENCES

1. C. V. Raman and K. S. Krishnan, "A new type of secondary radiation," Nature **121**, 501–502 (1928).
2. G. S. Landsberg and L. I. Mandelshtam, "Eine neue Erscheinung bei der Lichtzerstreuung in Krystallen," Naturwiss. **16**, 557–558 (1928).
3. K. J. Vahala, "Optical microcavities," Nature **424**, 839–846 (2003).
4. A. B. Matsko and V. S. Ilchenko, "Optical resonators with whispering-gallery modes—part I: basics," IEEE J. Sel. Top. Quantum Electron. **12**, 3–14 (2006).
5. S. Uetake, R. S. D. Sihombing, and K. Hakuta, "Stimulated Raman scattering of a high-*Q* liquid-hydrogen droplet in the ultraviolet region," Opt. Lett. **27**, 421–423 (2002).
6. V. S. Ilchenko, A. A. Savchenkov, A. B. Matsko, and L. Maleki, "Nonlinear optics and crystalline whispering-gallery-mode cavities," Phys. Rev. Lett. **92**, 043903 (2004).
7. O. Boyraz and B. Jalali, "Demonstration of a silicon Raman laser," Opt. Express **12**, 5269–5273 (2004).
8. T. J. Kippenberg, S. M. Spillane, B. Min, and K. J. Vahala, "Theoretical and experimental study of stimulated and cascaded Raman scattering in ultrahigh-*Q* optical microcavities," IEEE J. Sel. Top. Quantum Electron. **10**, 1219–1228 (2004).
9. I. S. Grudinin and L. Maleki, "Ultralow-threshold Raman lasing with CaF_2 resonators," Opt. Lett. **32**, 166–168 (2007).
10. I. S. Grudinin, A. B. Matsko, and L. Maleki, "On the fundamental limits of *Q* factor of crystalline dielectric resonators," Opt. Express **15**, 3390–3395 (2007).
11. I. S. Grudinin, V. S. Ilchenko, and L. Maleki, "Ultrahigh optical *Q* factors of crystalline resonators in the linear regime," Phys. Rev. A **74**, 063806 (2006).
12. A. A. Savchenkov, I. S. Grudinin, A. B. Matsko, D. Strekalov, M. Mohageg, V. S. Ilchenko, and L. Maleki, "Morphology-dependent photonic circuit elements," Opt. Lett. **31**, 1313–1315 (2006).
13. V. S. Ilchenko, X. S. Yao, and L. Maleki, "Pigtailing the high-*Q* microsphere cavity: a simple fiber coupler for optical whispering-gallery modes," Opt. Lett. **24**, 723–725 (1999).
14. E. D. Black, "An introduction to Pound–Drever–Hall laser frequency stabilization," Am. J. Phys. **69**, 79–87 (2001).
15. M. L. Gorodetsky and V. S. Ilchenko, "Optical microsphere resonators: optimal coupling to high-*Q* whispering-gallery modes," J. Opt. Soc. Am. B **16**, 147–154 (1999).
16. D. R. Rowland and J. D. Love, "Evanescent wave coupling of whispering-gallery-modes of a dielectric cylinder," IEE Proc.-J: Optoelectron. **140**, 177–188 (1993).
17. A. B. Matsko, A. A. Savchenkov, R. J. Letargad, V. S. Ilchenko, and L. Maleki, "On cavity modification of stimulated Raman scattering," J. Opt. B: Quantum Semiclassical Opt. **5**, 272–278 (2003).
18. A. B. Matsko, A. A. Savchenkov, N. Yu, and L. Maleki, "Whispering-gallery-mode resonators as frequency references. I. Fundamental limitations," J. Opt. Soc. Am. B **24**, 1324–1335 (2007).